Environ. Sci. Technol. **2006**, *40,* 1062−1068

Procedure for Determining Maximum Sustainable Power Generated by Microbial Fuel Cells

JOSEPH MENICUCCI,[†,⊥] HALUK BEYENAL,[†] ENRICO MARSILI,[†,‡] RAAJARAAJAN ANGATHEVAR VELUCHAMY,[†] GOKSEL DEMIR,[†,§] AND ZBIGNIEW LEWANDOWSKI*[,†,∥]

Center for Biofilm Engineering and Departments of Civil Engineering and Chemical and Biological Engineering, Montana State University, P.O. Box 173980, Room 366 EPS, Bozeman, Montana 59717-3980, Department of Chemical Engineering, University "La Sapienza", Via Eudossiana, 18 00184 Rome, Italy, and Department of Environmental Engineering, Faculty of Engineering, İstanbul University, Avcılar, 34320 İstanbul, Turkey

Power generated by microbial fuel cells is computed as a product of current passing through an external resistor and voltage drop across this resistor. If the applied resistance is very low, then high instantaneous power generated by the cell is measured, which is not sustainable; the cell cannot deliver that much power for long periods of time. Since using small electrical resistors leads to erroneous assessment of the capabilities of microbial fuel cells, a question arises: what resistor should be used in such measurements? To address this question, we have defined the sustainable power as the steady state of power delivery by a microbial fuel cell under a given set of conditions and the maximum sustainable power as the highest sustainable power that a microbial fuel cell can deliver under a given set of conditions. Selecting the external resistance that is associated with the maximum sustainable power in a microbial fuel cell (MFC) is difficult because the operator has limited influence on the main factors that control power generation: the rate of charge transfer at the current-limiting electrode and the potential established across the fuel cell. The internal electrical resistance of microbial fuel cells varies, and it depends on the operational conditions of the fuel cell. We have designed an empirical procedure to predict the maximum sustainable power that can be generated by a microbial fuel cell operated under a given set of conditions. Following the procedure, we change the external resistors incrementally, in steps of 500 Ω every 10, 60, or 180 s and measure the anode potential, the cathode potential, and the cell current. Power generated in the microbial fuel cell that we were using was limited by the anodic current. The anodic potential was used to determine the condition where the maximum sustainable power is obtained. The procedure is simple, microbial fuel cells can be characterized within an hour, and the results of the measurements can serve many purposes, such as: (1) estimating power generation in various MFCs, (2) comparing power generation in MFCs using different electroactive reactants, (3) quantifying the effects of the operational regime on the power generation in MFCs, and finally, (4) the purpose for which the procedure was designed, optimizing the performance of existing MFCs.

* Corresponding author phone: (406)994-5915; fax: (406)994-6098; e-mail: ZL@erc.montana.edu.

[†] Center for Biofilm Engineering, Montana State University.

[‡] University "La Sapienza".

[§] İstanbul University.

[∥] Department of Civil Engineering, Montana State University.

[⊥] Department of Chemical and Biological Engineering, Montana State University.

Introduction

The power generated by microbial fuel cells (MFCs) is computed as the product of the cell potential and the current in the external circuitry (*1*). The system (the fuel cell and the external circuit) is at a steady state if the power generated by the MFC equals the power consumption for an extended time. At steady state, the power production is sustainable. Because many steady states are possible, it is important to define conditions for which the sustainable current reaches a maximum and compute the maximum sustainable power that can be generated by a microbial fuel cell.

When the anode and the cathode of a fuel cell are connected through a resistor, current flows (*2*, *3*). The current is affected by the potential of the cell and by the electrical resistance. The electrical resistance has two components: external, the circuitry powered by the fuel cell, and internal, the fuel cell itself (*4*). Initially, before the external circuit is connected to the cell, the potential of the cell reflects the thermodynamic equilibriums of the anodic and cathodic reactions. If the external circuitry has a relatively low electrical resistance, then the equilibrium potential of the cell initially generates a high instantaneous electric current, higher than the maximum sustainable rate of charge transfer to/from the current-limiting electrode. As a result, the potential across the cell decreases quickly and adjusts to the rate of charge transfer to the current-limiting electrode, effectively decreasing the current in the external circuitry. However, if the external circuitry has a relatively high electrical resistance, then the equilibrium potential of the cell generates an electric current lower than the maximum sustainable rate of charge transfer to/from the current-limiting electrode. The potential of the cell adjusts to the external resistance. In the latter case, the power generation is sustainable but lower than it could be if the resistance of the external circuit was lower.

Each factor involved in the computation of power generated by a MFC—the cell potential and the current—depends on many other factors, such as the chemistry, concentrations of the reactants, and microbial activity, and some of these factors cannot be controlled by the operator (*5*−*7*). The cell can generate maximum power for a specific combination of external and internal resistances only. The external resistance can be controlled by the operator, but the internal resistance is an inherent feature of the fuel cell, and the operator cannot control it. Predicting the lowest external resistance at which the MFC yields the maximum sustainable power (MSP) from the circuit analysis is difficult because many factors affecting the internal resistance are difficult to quantify.

Most researchers studying MFCs make a point of estimating the power generated by these devices; some just measure the current by applying an arbitrarily selected external resistance and measuring instantaneous current and potential difference. Such instantaneous measurements estimate the power generated at the time of the measurement, but such data cannot be used to determine the maximum

10.1021/es051180l CCC: $33.50
Published on Web 12/27/2005

TABLE 1. Applied Resistor and Measured Current Values Found in Contemporary MFC Literature

Reference	Applied Resistor (Ω)	Measured Current (or Current Density)[a]
Liu et al. (*16*)	70−5000	0.2−2.2 A/m^2
Man et al. (*5*)	1000	18−130 mA/m^2
Chang et al. (*17*)	10	5 mA
Chaudhuri and Lovley (*18*)	1000	(31 mA/m^2)
Jang et al. (*19*)	10−1000	2−0.4 mA
Bond and Lovley (*20*)	500	0.4 mA
Park and Zeikus (*21*)	300	14 mA
Lee et al. (*22*)	560	0.075−0.35 mA
Simon et al. (*23*)	not listed	(30−80 μA/cm^2)
Pizzariello et al. (*24*)	100 000	(5.94 μA/ cm^2)
Park et al. (*25*)	1000	0.08−0.22 mA
Kim et al. (*26*)	1000	0.04 mA

[a] Current densities are reported only if they are available.

sustainable power. Also, this approach does not allow for the comparison of various devices and various operational procedures because the choice of the external resistor is arbitrary, and the power generated by the fuel cell is consistent with that choice. Table 1 shows a selection of such measurements extracted from the available literature.

To compare the power generated in various MFCs, it is useful to start by standardizing the method of measuring the power, so that the results and the fuel cells can be compared. Selecting the external resistor is the most important task in evaluating the power generated by a MFC, and it is the key to determining the sustainable power generated by the MFC (*8*). Once the electrodes are connected through an external resistor, the cell potential decreases because of the limitations imposed on the electrode reaction kinetics, on mass transfer, and on charge-transfer processes at the current-limiting electrode (the one of the two electrodes that exhibits the slower charge-transfer kinetics). The decreasing cell potential decreases the current flowing through the external circuit, following Ohm's equation, $I = V/R$. Figure 1 illustrates the factors affecting the power generated by MFCs.

The power generated by the MFC is limited by (1) the charge-transfer resistance to the electrode including kinetic or mass transfer limitations or (2) the external resistance. The effect of the internal mass transfer resistance is well-known and is easy to understand. It can be demonstrated by stirring the solution of electroactive species to increase convection and the current. The effect of the external resistance on the power generated by the MFC is more complex and can be visualized by short-circuiting the electrodes, which forces the cell to generate high power for a very short time. Such elevated power generation is not sustainable, and it decreases rapidly in time. This effect highlights the need for a procedure to select the "correct" resistance for determining the power generated by microbial fuel cells.

The goal of this paper is to develop a procedure for selecting the external resistance for microbial fuel cells that ensures generation of the MSP. To demonstrate the utility of this procedure, we have designed and operated a MFC using *Klebsiella pneumoniae* oxidizing glucose in the anodic compartment and the abiotic reduction of oxygen in the cathodic compartment. The resistor for which the cell generated MSP was selected empirically by changing the resistances at a predefined rate (ohms per unit time) and measuring potentials and currents.

Materials and Methods

Microbial Fuel Cell Components. The microbial fuel cell used in our experiments is shown in Figure 2. The cell casing was made out of polycarbonate and had anodic and cathodic compartments separated by a cation exchange membrane ESC-7000 (Electrolytica Corporation, 770-410-9166). Each chamber had a working volume of 250 mL. A saturated calomel electrode was used as a reference electrode (Fisher, catalog no. 13-620-51) and was located in the cathodic chamber of the MFC. J-cloths with thicknesses of 0.1 mm (First Brands Corporation), which were located in front of the cation exchange membrane, were used to protect the cation exchange membrane from direct contact with the electrodes and to minimize microbial growth on the cation exchange membrane (*2*, *9*). Feed and effluent tubing was made of Neoprene (Cole-Parmer, catalog no. 148441). Glass flow breakers located in feed lines were used to prevent contamination.

Anodic Compartment. In the anodic compartment, glucose is oxidized anaerobically by *Klebsiella pneumoniae* (ATCC no. 700831) according to the following reaction

$$C_6H_{12}O_6 + 6H_2O \rightarrow 6CO_2 + 24H^+ + 24e^- \quad (1)$$

The microbial growth medium in the anodic compartment had the following composition: 10 g/L tryptone, 5 g/L yeast extract, 5 g/L sodium chloride, 9.12 g/L Na_2HPO_4, 1.75 g/L KH_2PO_4, and 1 g/L glucose. Equation 1 illustrates the principle of extracting electrons from organic substances. The growth medium used in the MFC is a complex solution of nutrients, and not only glucose but also organics in yeast extract and tryptone are oxidized by the microorganisms. The anode was made of reticulated vitreous carbon (RVC) connected to graphite rods (Sigma-Aldrich, CAS no. 7782-42-5). The anodic surface area for the 80-ppi RVC was approximately 0.4 m^2, calculated from the specifications given by the vendor.

Cathodic Compartment. The cathodic reaction was the reduction of oxygen. The electrode potential, at standard conditions, of the cathode was reported as 0.16 V_{SCE} for the following reaction

$$O_2 + 2H_2O + 4e^- \rightarrow 4OH^- \quad (2)$$

The air electrode was used as the cathode. It was provided courtesy of Dr. Neal Naimer of the Electric Fuel Corporation of the Arotech Corporation (*11*). The electrode was composed of two active layers of carbon bonded to each side of a current-collecting screen made of nickel mesh (*12*). The electrode uses oxygen in the gas or liquid phase and reduces it on the electrode surface.

To prevent the pH from changing in the cathodic compartment, we used a phosphate buffer (1.825 g/L of Na_2HPO_4 and 0.35 g of KH_2PO_4) at a pH of 7.2. The surface area of the cathode was 79 cm^2 (measured).

Fuel Cell Startup and Operating Conditions. Preparation of Inoculum. One mL of a frozen stock culture of *K. pneumoniae* was added to 100 mL of medium and was allowed to grow overnight (18 h) at room temperature on a rotary shaker (150 rpm).

MFC Preparation. The microbial fuel cell was cleaned thoroughly in deionized water. The cation exchange membrane was soaked in 1 M NaCl for at least 24 h before installing in the cell. The cell was assembled as shown in Figure 2. Both compartments were filled with deionized water (used to avoid dry autoclaving). A rubber stopper was used to protect the open port (used to house the reference electrode). The MFC was autoclaved at 121 °C for at least 20 min. The rubber stopper was removed, and a saturated calomel electrode (SCE) was inserted. The water in the anodic and cathodic compartments was drained, and the growth medium was pumped into the anodic compartment of the cell while phosphate buffer was pumped into the cathodic compartment of the fuel cell.

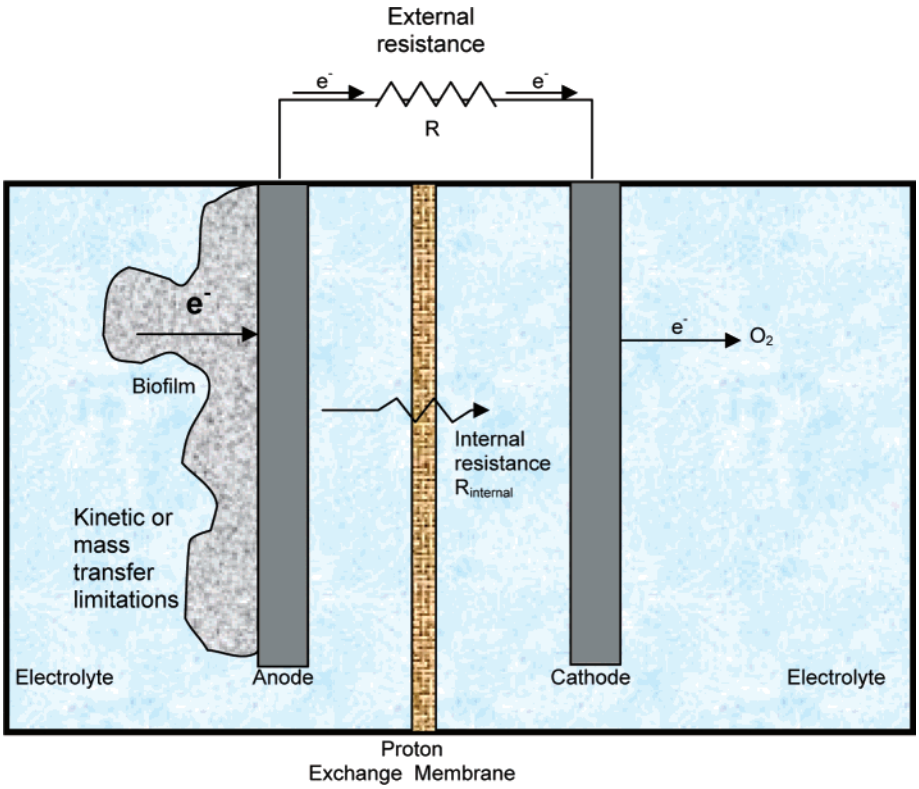

FIGURE 1. Simplified charge transfer in an MFC depicting factors affecting the external and internal resistances.

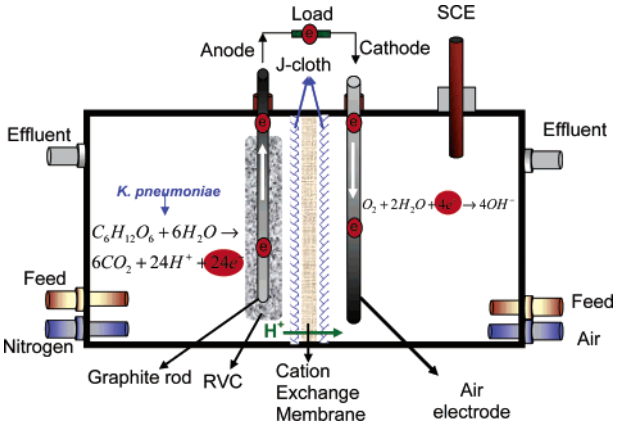

FIGURE 2. Microbial fuel cell used in the experiments (*9*).

Then, 60 mL of the *K. pneumoniae* stock culture was inoculated into the cell, replacing 60 mL of the sterile medium. The bacteria were allowed to grow in batch mode until the anodic potential stabilized (~−450 mV_{SCE}). Sterile medium was then pumped into the anodic compartment at a flow rate of 0.3 mL/min for the duration of the experiments.

Measurement of Anodic and Cathodic Potentials and Current in a Microbial Fuel Cell. The anodic and cathodic potentials of our microbial fuel cell were measured against a saturated calomel electrode (Fisher, catalog no. 13-620-51) using a data logger (HP model no. 34970A) to store the measured values regularly (every 10 s). A variable resistance box (Ohm-Ranger, Ohmite Manufacturing Co.) was used to select an applied external resistance for current measurement. Figure 3 shows the circuit diagram for logging the current and the anodic and cathodic potentials. The circuit consists of two different wiring sections: one for the potential measurement and one for the current measurement. For the current measurement, the anode and the cathode are connected to the current channel through a variable resistor box in series. For potential measurement, the anode and cathode are connected to potential channels 1 and 2 of the data logger, respectively, with the SCE connected to the common terminal of the potential channels.

Evaluating Sustainable Power. To evaluate the sustainable power, we applied a decreasing resistance at a predefined scan rate and measured the current and cell potentials for each resistance. Later, the applied resistor, cell potential, and current were used to calculate power, and we then evaluated sustainable power from the results of these measurements as shown below.

Example of Measurements and Computations. An example measurement showing how current and cell potential change with the external resistance is shown in Figure 4. The external resistance was changed stepwise in equal time intervals. For practical reasons, we used an approximation to describe this steplike variation as a continuous change of resistance with respect to time ($dR/dt = 0.5\ k\Omega/min$, shown by a dashed line).

The data used to predict sustainable power were produced after the MFC reached a stable cell potential (~550 mV). The different resistances were applied using an external resistor-ranger (Ohm-Ranger, Ohmite Manufacturing Co.). The initial external resistance was 10 kΩ, and the resistance was decreased by 0.5 kΩ every minute (called the resistance scan rate) until we reached 0.5 kΩ. The average current value at each external resistance (over one minute) was used to calculate power.

Using the initial anodic potential ($E_{o,anodic}$) and anodic potentials at each applied external resistance, we calculated the relative decrease in anodic potential as follows

$$\text{relative decrease in anode potential (\%)} = \frac{E_{o,anodic} - E_{anodic}}{E_{o,anodic}} \times 100 \quad (3)$$

The relative decrease in anode potential (RDAP) is used to evaluate maximum sustainable power.

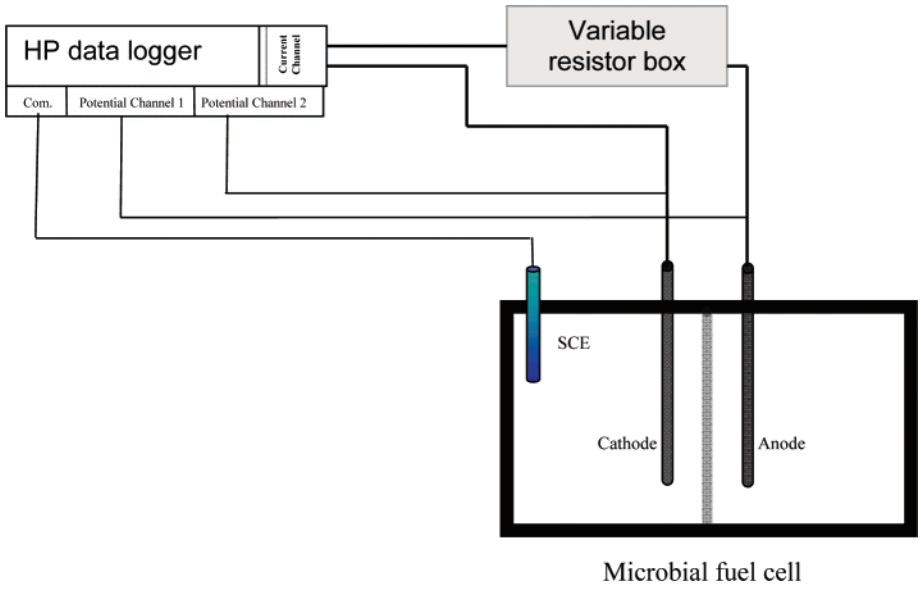

FIGURE 3. Circuit diagram for logging the current and the anodic and cathodic potentials.

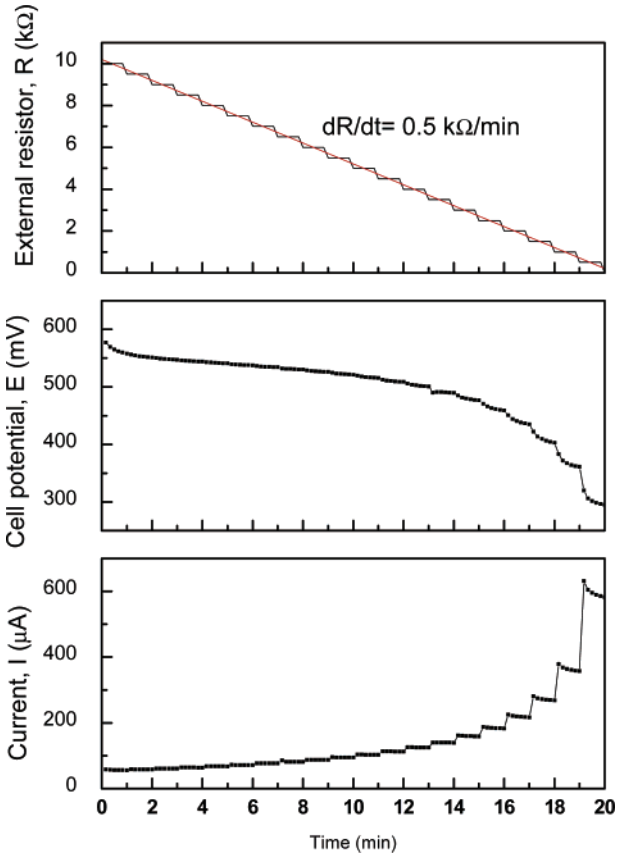

FIGURE 4. Resistance scan shows the effect of applied external resistance on the variations of cell potential (*E*, potential difference between anode and cathode) and current (*I*). The continuous line is an approximation of the stepwise ramp of the decreasing resistance (d*R*/d*t* = 0.5 kΩ/min).

Effect of the External Resistance Scan Rate on the Sustainable Power. We repeated the measurements in Figure 4 starting at an initial external resistance of 10 kΩ. We tested external resistance scan rates of 0.5 kΩ/10 s, and 0.5 kΩ/180 s.

Experimental Verification of the Computed Maximum Sustainable Power. To verify that the maximum sustainable power computed using our technique is consistent with the sustainable power evaluated by operating microbial fuel cells, we operated a microbial fuel cell for weeks, applying different resistors to verify the evaluated sustainable power. The resistances selected were 6, 5, 4, 3.5, 3, 2.5, 2, 1.5, 1, 0.5, 0.25, and 0.125 kΩ. We then operated our microbial fuel cell for a long time period (generally greater than 6 h), applying a single constant resistance, and measured the current and anodic and cathodic potentials with respect to time.

Results and Discussion

From the data in Figure 4 we plotted potentials of the cathode (Figure 5A), anode (Figure 5B), and cell (Figure 5C) and the relative decrease in anode potential (Figure 5D) against the external resistance. The cathodic potential was constant (Figure 5A) at each external resistance, showing that the current is limited by the anode (*13*). The cell potential decreased significantly when we applied a resistance less than 3 kΩ (Figures 5B and 5C).

We used the relative decrease in anodic potential (RDAP) to select the external resistor to measure the maximum sustainable power of our microbial fuel cell (Figure 5D). When external resistance is high, the RDAP increases linearly with decreasing external resistance because the electron delivery to the cathode is limited by external resistance (region B in Figure 5D). However, when a low external resistance is applied, the electron delivery to the cathode is limited by kinetic and/or mass transfer (or internal resistance) (region A in Figure 5D), and the RDAP increases linearly with decreasing external resistance. However, the RDAP increases linearly with decreased external resistance, with different slopes, for external resistance limited or internal resistance limited conditions (Figure 5D). The conditions where external and internal resistance limitations are equal must be somewhere between these two lines, which is presented as a shaded area in Figure 5D (resistances between 2.5 and 4 kΩ). When line A and line B intersect, we draw a horizontal line from the intersection to estimate the external resistor that allows us to measure sustainable power. Our experiments showed that any external resistance between 2.5 and 4 kΩ provides very close power values (less than 20% difference between them, so that the selection of an external resistor between 2.5 and 4 kΩ does not produce a significant error on predicted sustainable power), but only the power generated when a 4 kΩ resistor was used remained constant for long period of time. Although our graphical procedure predicted a 3.5 kΩ resistor to obtain sustainable power, we

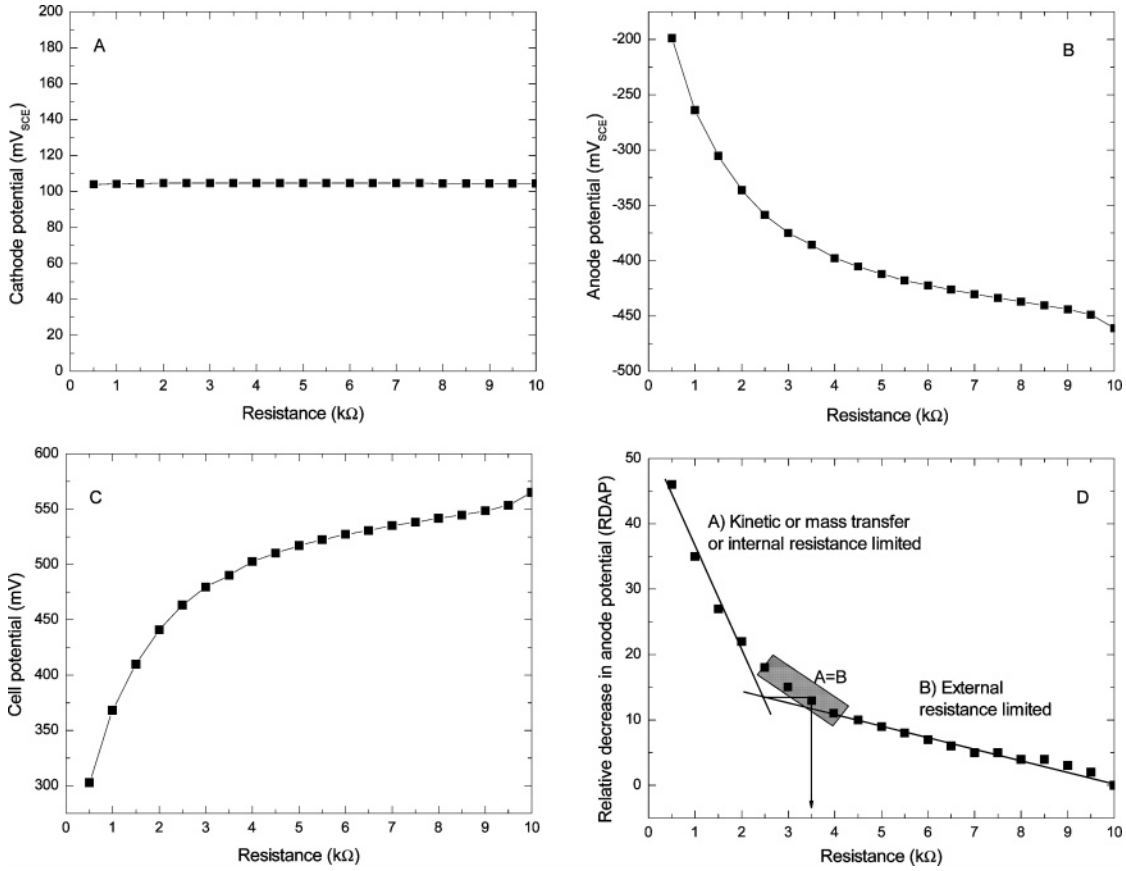

FIGURE 5. Effect of external resistance on the (A) cathodic, (B) anodic, and (C) cell potentials. Anodic and cathodic potentials are presented against a saturated calomel electrode (SCE). The resistance scan rate was 500 Ω/60 s in all experiments. (D) The variation of percent deviation of anodic potential with respect to applied external resistance. The linear fit at high external resistances (region B) represents a region in which the external resistance controls the power. The linear fit at low external resistances (region A) represents a region in which the power is limited by kinetics, mass transfer, or internal resistance.

TABLE 2. Effect of the Rate of Change of External Resistance on the Change in Sustainable Power[a]

Rate of Change of Resistance (kΩ/time)	Evaluated Maximum Sustainable Power (μW)	Corresponding Resistor (kΩ)
0.5 kΩ/10 s	86	3 kΩ
0.5 kΩ/60 s	68	3.5 kΩ
0.5 kΩ/180 s	69	3.5 kΩ

[a] Although from the given graphical procedure we found an external resistor value of 3−3.5 kΩ that corresponds to a sustainable power, experimentally we used a slightly higher external resistor (4 kΩ) to be sure that the power is sustainable.

noticed that there was not any significant difference in powers when we use 3.5 or 4 kΩ resistors (less than 10% difference), so we decided to select 4 kΩ to measure power of our microbial fuel cell by considering variations in microbial activities in the fuel cell.

The resistance scan was started from a resistance of 10 kΩ (Figures 4 and 5). We repeated the same measurements (as shown in Figure 4) starting from 70 kΩ and identified the same maximum sustainable power (results not shown).

Effect of External Resistance Scan Rate on the Evaluated Sustainable Power. Table 2 shows the evaluated sustainable power and corresponding external resistance for different resistance scan rates (0.5 kΩ/10 s, 0.5 kΩ/60 s, 0.5 kΩ/180 s). For lower external resistance scan rates, the difference between predicted maximum sustainable power is very small (1 μW). However, there is a 20% difference in the predicted maximum sustainable powers between 0.5 kΩ/10 s and 0.5 kΩ/60 s external resistance scan rates. This difference in predicted maximum sustainable powers also justifies that our selection of applied external resistance to measure maximum sustainable power must be slightly higher from the graphically predicted one.

Experimental Verification of the Evaluated Sustainable Power. The maximum sustainable power of our microbial fuel cell was evaluated from a 30 min experiment. This sustainable power is 65.51 μW, which was measured using a 4 kΩ resistor. If this prediction is correct, then a resistance value less than 4 kΩ should cause a drop in cell current with time. However, any resistance greater than 4 kΩ should not change the cell current; the current should remain constant with respect to time. Figure 6 shows the temporal variation of cell current for three applied external resistors: (1) an external resistance less than the resistance able to maintain a corresponding sustainable current or power (0.25 kΩ), (2) an external resistance able to maintain a corresponding sustainable current or power (4 kΩ), and (3) an external resistance that consumes less current or power than the cell produces (6 kΩ). When we used a 0.25 kΩ resistor, there was a significant, immediate, and continuous drop in current and cell potential, while current and potential remained constant over many hours when we used a 4 kΩ resistor. When we used a 6 kΩ resistor, the cell current was below maximum sustainable current.

We operated our microbial fuel cell for over 2 weeks, applying various external resistances to verify the evaluated sustainable power. We found that any resistance less than that able to yield a corresponding maximum sustainable current and power lowered the cell potential and current for

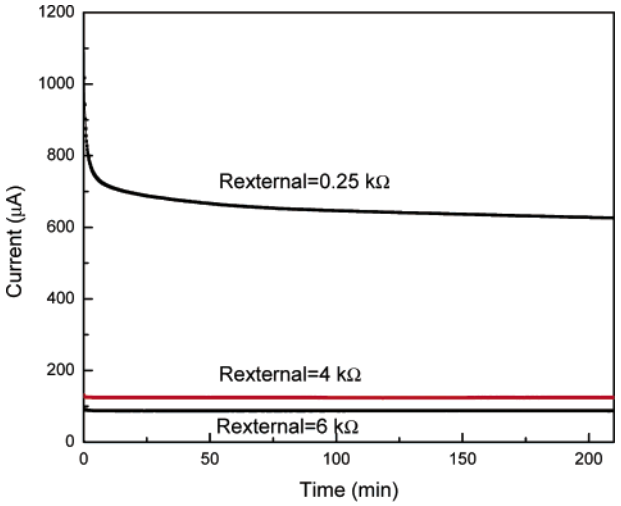

FIGURE 6. Current measured over 200 min for 0.25, 4, and 6 kΩ external applied resistances. The current remains constant when a 4 or 6 kΩ resistance is applied. However, the current decreases with respect to time when a 0.25 kΩ resistance is applied.

TABLE 3. Rate of Change of Cell Potential in a Microbial Fuel Cell

Resistor	Slope (mV/min)
0.125 kΩ	−0.24 ± 0.23
4 kΩ	−0.02 ± 0.05
6 kΩ	−0.03 ± 0.09

a minimum of 4 h but that any resistance at or above the resistance able to yield a corresponding sustainable current and power did not change the cell potential and maintained constant power. We then operated our microbial fuel cell for 16 h, applying a 4 kΩ resistance, and found that current and cell potential remained constant. This verified our sustainable power predictions (performed within less than 30 min).

Table 3 shows the calculated slopes (temporal variation of cell potentials) of the lines in Figure 6 between 5 and 200 min (calculated for every 30 min). A zero slope shows that cell potential does not change with time, and a slope with a magnitude lower than zero indicates that the cell potential does change with time; the value shows the rate of the change.

Comparing the Maximum Sustainable Power with the Maximum Power. The definition of sustainable power implies that the power generated does not change with time and the cell potential remains constant after applying the external resistance. However, the sustainable power obtained using higher resistances may be less than the maximum sustainable power, as shown in Figure 7. The sustainable power measurement at a resistance of 4 kΩ was 61.51 μW. The measurements in Figure 7 were taken 1 h after applying the external resistance. Figure 7B shows that even after 1 h the power in a microbial fuel cell continues to decrease when the resistance is less than that which can maintain a sustainable resistance.

The results in Figure 8 show that the power generated by the MFC depended on the resistor, if the power was not sustainable, as expected. The power also depended on the time that the cell was allowed to equilibrate, which demonstrates the transitional conditions and nonsustainable power generation. Only when the external resistance was large enough did the power generation reach a sustainable level quickly. The lower the external resistance, the longer the time needed for the cell to equilibrate and produce the sustainable power. When a large, 6 kΩ, resistor was used, power generation was at a steady state after 10 s.

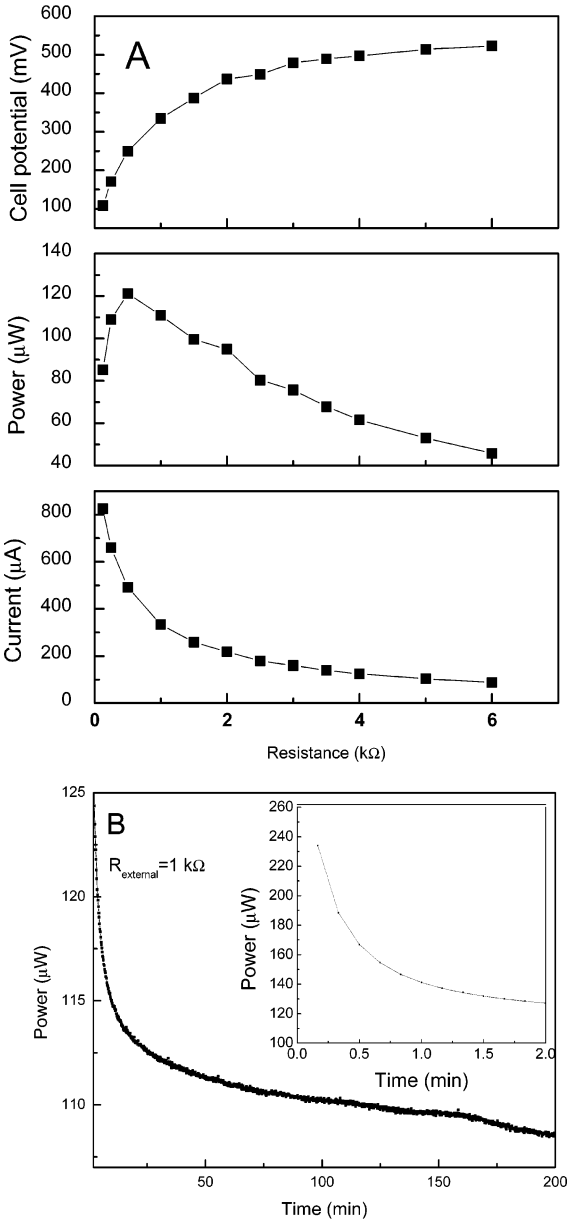

FIGURE 7. (A) Current, cell potential, and power measurements in a microbial fuel cell (measured at $t = 1$ h). (B) Power measurements in a microbial fuel cell with an applied external resistance of 1 kΩ. Note that power continues to decrease even after 300 min of continuous operation.

From Figure 8, the maximum power of the MFC was estimated as 395 μW. However, the maximum sustainable power of the microbial fuel cell was only 65 μW, much smaller (6 times) than the maximum power. Similar to our study, He et al. recently measured the power of their microbial fuel cell and reported the maximum power that occurred when a 66 Ω resistor was applied (*14*). However, when they applied a larger resistor, 100 Ω, the current decreased in time (Figure 3 in their paper). When they applied a 470 Ω resistor, the current did not change, showing the sustainable conditions. These results corroborate our observations. In another study, Schroder et al. changed the external resistance and measured maximum power (similar to Figure 8) but did not test whether the measured maximum was sustainable (*15*).

Note that the resistance corresponding to the sustainable power evaluated from Figure 5D can be roughly estimated from Figure 8. However, this takes a significantly longer time (more than 12 h) and gives a rough estimate only. The

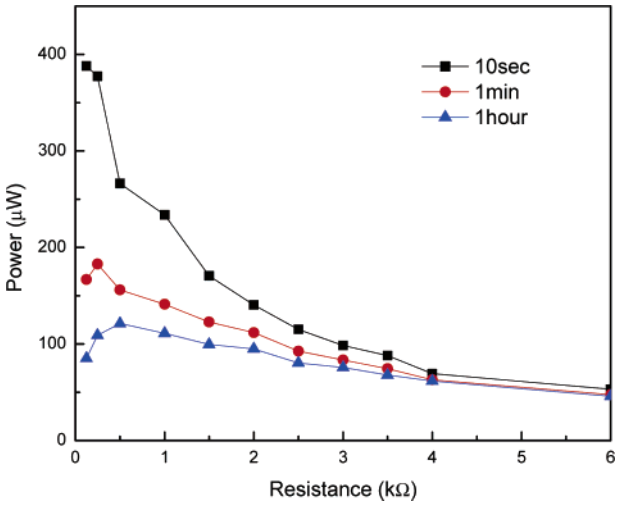

FIGURE 8. Power generated by the MFC was measured using various external resistors. The power generated by the cell changes with time, demonstrating unstable conditions and nonsustainable power generation. Only when a high resistor is used does the cell reach a steady state quickly; it produces steady-state power after just 10 s.

procedure developed in this paper evaluates the maximum sustainable power in less than 30 min, highlighting its easiness.

The procedure for evaluating the sustainable power generated by microbial fuel cells can be executed in a short time (less than 1 h), and the results have been verified in long-term experiments (lasting more than 2 weeks).

The maximum sustainable power generated by microbial fuel cells can be used to report the cell performance under a defined set of operational conditions. Microbial fuel cells characterized by maximum sustainable power can be compared to each other.

Acknowledgments

The authors gratefully acknowledge the financial support provided by the United States Office of Naval Research, contract no. N00014-02-1-0567. The authors also thank Dr. Neal Naimer and Jonathan Sassen of Electric Fuel Ltd. for their contributions to this research. Goksel Demir was supported by the Scientific and Technical Research Council of Turkey, Directorate of Human Research Development, project no. 1452-4140 NATO B1.

Literature Cited

(1) Liu, H.; Cheng, S.; Logan, B. E. Power generation in fed-batch microbial fuel cells as a function of ionic strength, temperature, and reactor configuration. *Environ. Sci. Technol.* **2005**.

(2) Bennetto, H. P.; Stirling, J.; Delaney, G.; Roller, S.; Thurston, C. S.; Mason, J. R. Microbial fuel-cells. *Process Biochem.* **1983**, *18* (4), R17.

(3) Allen, R. M.; Bennetto, P. H. Microbial fuel cells: Electricity production from carbohydrates. *Appl. Biochem. Biotechnol.* **1993**, *39*, 27−40.

(4) Grzebyk, M.; Pozniak, G. Microbial fuel cells (MFCs) with interpolymer cation exchange membranes. *Sep. Purif. Technol.* **2005**, *41* (3), 321−328.

(5) Man, B.; Cheng, S.; Logan, B. E. Electricity generation using membrane and salt bridge microbial fuel cells. *Water Res.* **2005**, *39*, 1675−1686.

(6) Rabaey, K.; Verstraete, W. Microbial fuel cells: Novel biotechnology for energy generation. *Trends Biotechnol.* **2005**, *23* (6), 291−298.

(7) Zhang, X. C.; Halme, A. Modeling of a microbial fuel-cell process. *Biotechnol. Lett.* **1995**, *17* (8), 809−814.

(8) Rabaey, K.; Ossieur, W.; Verhaege, M.; Verstraete, W. Continuous microbial fuel cells convert carbohydrates to electricity. *Water Sci. Technol.* **2005**, *52* (1−2), 515−523.

(9) Rhoads, A.; Beyenal, H.; Lewandowski, Z. Microbial fuel cell using anaerobic respiration as an anodic reaction and biomineralized manganese as a cathodic reactant. *Environ. Sci. Technol.* **2005**, *39* (12), 4666−4671.

(10) Bard, A. J.; Faulkner, L. R. *Electrochemical Methods: Fundamentals and Applications*, 2nd ed.; John Wiley and Sons: New York, 2001.

(11) Putt, R.; Naimer, N.; Koretz, B. Advanced Zinc−Air Primary Batteries. In *Proceedings of the 39th Power Sources Conference*, Cherry Hill, NJ, 2000.

(12) Hamlen, R. P.; Atwater, T. B. In *Handbook of Batteries*, 3rd ed.; Linden, D.; Reddy, T. B., Eds.; McGraw-Hill: New York, 2002.

(13) Sawyer, D. T.; Heineman, W. R.; Beebe, J. M. *Chemistry Experiments for Instrumental Methods*; John Wiley and Sons: New York, 1984.

(14) He, Z.; Minteer, S. D.; Angenent, L. T. Electricity generation from artificial wastewater using an upflow microbial fuel cell. *Environ. Sci. Technol.* **2005**, *39* (14), 5262−5267.

(15) Schröder, U.; Nieben, J.; Scholz, F. A generation of microbial fuel cells with current outputs boosted by more than one order of magnitude. *Angew. Chem., Int. Ed.* **2003**, *42* (25), 2880−2883.

(16) Liu, H.; Cheng, S.; Logan, B. E. Production of electricity from acetate or butyrate using a single-chamber microbial fuel cell. *Environ. Sci. Technol.* **2005**, *39*, 658−662.

(17) Chang, I. S.; Jang, J. K.; Gil, G. C.; Kim, M.; Kim, H. J.; Cho, B. W.; Hong, K. B. Continuous determination of biochemical oxygen demand using microbial fuel cell type biosensor. *Biosens. Bioelectron.* **2004**, *19*, 607−613.

(18) Chaudhuri, S. K.; Lovley, D. R. Electricity generation by direct oxidation of glucose in mediatorless microbial fuel cells. *Nat. Biotechnol.* **2003**, *21* (10), 1229−1232.

(19) Jang, J. K.; Pham, T. H.; Chang, I. S.; Kang, K. H.; Moon, H.; Cho, K. S.; Kim, B. H. Construction and operation of a novel mediator- and membrane-less microbial fuel cell. *Process Biochem.* **2004**, *39* (8), 1007−1012.

(20) Bond, D. R.; Lovley, D. R. Electricity production by *Geobacter sulfurreducens* attached to electrodes. *Appl. Environ. Microbiol.* **2003**, *69* (3), 1548−1555.

(21) Park, D. H.; Zeikus, J. G. Improved fuel cell and electrode designs for producing electricity from microbial degradation. *Biotechnol. Bioeng.* **2003**, *81* (3), 348−355.

(22) Lee, S. A.; Choi, Y.; Jung, S.; Kim, S. Effect of initial carbon sources on the electrochemical detection of glucose by *Gluconobacter oxydans*. *Bioelectrochemistry* **2002**, *57*, 173−178.

(23) Simon, E.; Halliwell, C. M.; Toh, C. S.; Cass, A. E. G.; Bartlett, P. N. Oxidation of NADH produced by a lactate dehydrogenase immobilised on poly(aniline)−poly(anion) composite films. *J. Electroanal. Chem.* **2002**, *538*−*539*, 253−259.

(24) Pizzariello, A.; Stredánsky, M.; Miertus, S. A glucose/hydrogen peroxide biofuel cell that uses oxidase and peroxidase as catalysts by composite bulk-modified bioelectrodes based on a solid binding matrix. *Bioelectrochemistry* **2002**, *56*, 99−105.

(25) Park, H. S.; Kim, B. H.; Kim, H. S.; Kim, H. J.; Kim, G. T.; Kim, M.; Chang, I. S.; Park, Y. K.; Chang, H. I. A novel electrochemically active and Fe(III)-reducing bacterium phylogenetically related to *Clostridium butyricum* isolated from a microbial fuel cell. *Anaerobe* **2001**, *7* (6), 297−306.

(26) Kim, H. J.; Park, H. S.; Hyun, M. S.; Chang, I. S.; Kim, M.; Kim, B. H. A mediator-less microbial fuel cell using a metal reducing bacterium, *Shewanella putrefaciens*. *Enzyme Microb. Technol.* **2002**, *30* (2), 145−152.

Received for review June 21, 2005. Revised manuscript received November 14, 2005. Accepted November 15, 2005.

ES051180L